euspen's 20th International Conference & Exhibition, Geneva, CH, June 2020
www.euspen.eu

Technological investigation for production of metallic micro-optics employing embossing process

D. A. Rolón[1], M. Jagodzinski[1], S. Kühne[1], S. Gebauer[1], M. Malcher[1], D. Oberschmidt[1]

[1]*Berlin Institute of Technology, department of Micro and Precision devices MFG, Germany*

rolon@mfg.tu-berlin.de

Abstract
Micro optics are well established in today's world, from the high-tech sector to the broad consumer market. They enable new optical functionalities, optimized beam shaping and light utilization with a simultaneous weight advantage and the associated conservation of resources. The constantly increasing integration density and speed of innovation present a challenge for the economical production of such optics. The production of optical structures in molding tools by means of ultra-precision machining is carried out individually and requires considerable effort in terms of production time and machine requirements. The effort increases when arrays or large-area diffractive optics are manufactured. Lithographic processes such as interference lithography are established for the production of optical arrays. However, the time advantage of this process is at the expense of reduced freedom of form. A barely described alternative is to form ultra-precision optics into metallic surfaces. This technique offers the potential to efficiently produce both original individual components up to small batches as well as master structures for replication. Moreover, this process has less expenses as well as enhanced freedom of form. This paper consists of a technological investigation for the production of micro optics (arrays) in aluminum RSA-501 and gold layers by embossing using plunger coil actuators. Moreover, a parameter investigation to assess the influence of the embossing force, load time and embossing speed on the micro optic geometry was conducted. The experiments were performed using a fast-tool servo coupled with a force sensor and a ruby spherical embossing tool in a modified ultra-precision machine centre LT ULTRA MMC 1100. The experimental results indicate the relevance of the embossing force in contrast to the embossing speed, indicating that higher speeds could be applied during process to gain an increase in productivity. The process is proven to be feasible and successfully implemented for manufacturing micro-optic arrays (MOAs) in RSA-501 and gold.

Keywords : micro optic arrays, embossing, RSA-501, gold, forming

1. Introduction

Optical elements such as minituarized lenses enable a variety of recent applications. For instance, micro-optical arrays (MOAs) containing a large number of lenslet cells is being used in a wide range of applications in cameras, sensors and other photonic devices. These MOAs provide a performance enhancement in a large visual field and miniaturized size.

Essentially, micro-optics (MO) are a few orders of magnitude above or below the application wavelength. These MOs enable to reach down to the nanometer range. Examples of applications can be found in optical arrays in honeycomb condensers, light conduction in displays, beam homogenization in laser and exposure systems. For efficient production, replication in polymers and glass using injection moulding or hot-embossing processes are extensively applied. Also, lithographic and machining processes compete in the production of the required form structures for replication [1].

Among the machining processes existing to manufacture high-quality MOs, ultra-precision on-axis or off-axis turning with single crystal diamond tools, also known as single point diamond turning (SPDT), is an established method. This process can also be enhanced by using a fast-tool- or slow-slide-servo system. Additionally, processes such as ultra-precision milling, flycutting and shaping process are also well established. Those processes are mainly carried out on specially designed ultra-precision machine tools based on the manufacturing technology of macroscopic optics. Also, single crystal diamond tools are still necessary for manufacturing non-ferrous metallic optical elements [2]. The SPDT process is the most common and standardized application regarding its process control [3, 4]. Brinksmeier et al. provide a comprehensive overview of MOs production [5]. Scheiding et al. compare the manufacturing process with regard to lens arrays on flat and curved surfaces using micro-milling process as well as the fast-tool- and slow-slide-servo [6]. Also Kirchberg et al. investigated the micro-milling process with diamond tools to produce micro-lens arrays (MLAs) [7].

The process parameters, surface development mechanisms and the suitability of materials have been extensively investigated with regard to the production of continuous surfaces. Lithographic methods such as interference lithography are time-advantage processes, however it is at expense of reduced freedom of form. The SPDT technique requires a suitable ultra-precision machine tool and expensive diamond tools. Also replication techniques are limited to polymer and glasses, therefore not including metallic MOAs. Therefore, this paper aims at investigating the usage of embossing process in gold (Au) and aluminum RSA-501 for manufacturing micro-optics.

2. Methodology

The experiments presented in this paper consisted of adapting a fast-tool-servo (FTS) from the company LT Ultra-Precision

TECHNOLOGY GMBH, Germany coupled with a tool holder in a modified ultra-precision machine center LT Ultra MMC 1100 from the company LT ULTRA-PRECISION TECHNOLOGY GMBH, Germany. By using a peak current I = 6.85 A, the maximum actuator force can be estimated at F_{max} = 102.6 N. The embossing tool axis and force are aligned to minimize other force components and momentum along the experiments. The advantage of fixing the embossing system in the ultra-precision machine-tool is that its axes (X,Y,Z) are able to move within a few nanometers of accuracy. Also, the whole experiment can be conducted within almost without external temperature influence. For measuring the embossing force, a piezoelectric force sensor was adapted between fast-tool servo system and tool holder.

The workpiece is positioned on the machine tool table, fixed using Crystalbond™ adhesive. The embossing experiments on gold and RSA-501 were done according to the scheme presented in Figure 1 where Z_s refers to the safety position, Z_{wp} the embossing position, v_Z the embossing speed, t the hold time, F_p the embossing force and Z = 0 is the contact position between tool and workpiece.

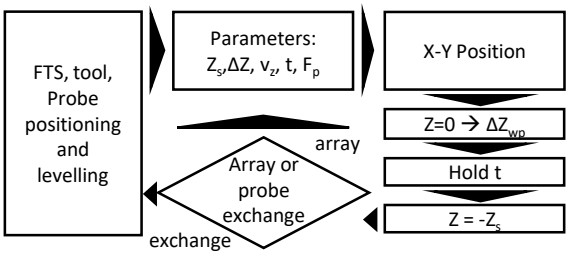

Figure 1. Scheme of the embossing procedure for gold and RSA-501

The workpiece surface is oriented orthogonally to the fast tool-servo system. In Figure 2 the set-up of the embossing system on the ultra-precision machine Z axis and an illustration of the embossing experiments are shown. The embossings were measured by means of a white light interferometer (WLI) ZYGO NEWVIEW 5010 from the company ZYGO CORPORATION, United States. For analysing the WLI measurements, the software GWYDDION was used.

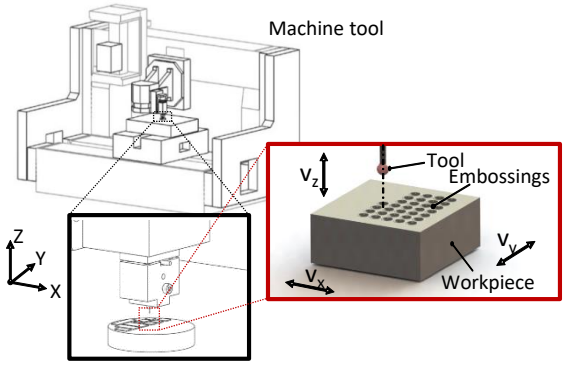

Figure 2. Process description and machine kinematic

2.1. Embossing device specification

The fast-tool servo (FTS) is based on an air bearing as guidance and a voice coiled actuator (VCA). The current signal to control the VCA is generated by a micro-controller coupled with an amplifier MOSFET IRL530NPbF.

The tool is fixed on the FTS forcer. In Figure 3 a 3-D model of the FTS used for the experiments is shown. The embossing force was measured using a force sensor 9131B from the company KISTLER GMBH, Switzerland. A scheme of the embossing process by moving the machine Z axis is depicted on Figure 4.

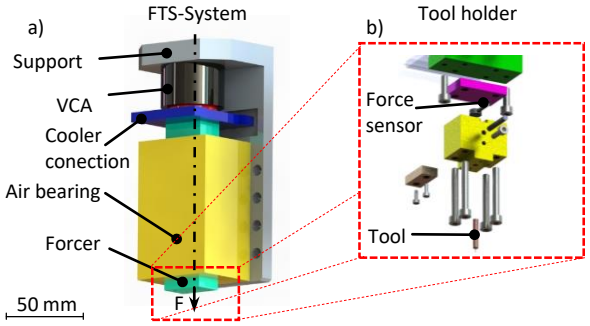

Figure 3. a) 3-D model of the fast-tool-servo used for the experiments b) Tool holder and coupled force sensor used

The FTS system is only indirectly associated with the embossing tool displacement during the experiments as the primary displacement consists of the machine Z axis movement of the ultra-precision machine LT-Ultra MMC 1100. The forcer mass of the FTS can be determined from the measurement series with pure weight force, at the current I = 0 A. The average rotor mass found was m = 331.8 g. The FTS also has two elastic stoppers made of plastic. The difference of the operating point and the machine current position in Z_s must be determined. The Z = 0, meaning the contact position between tool and workpiece, is stored as soon as the air bearing starts to free running, without contact with the FTS plastic stoppers. A safety distance between the contact point Z = 0 and the end stopper is set within a few milimiters Z_{wp}. The displacement of the tool is measured by a chromatic sensor.

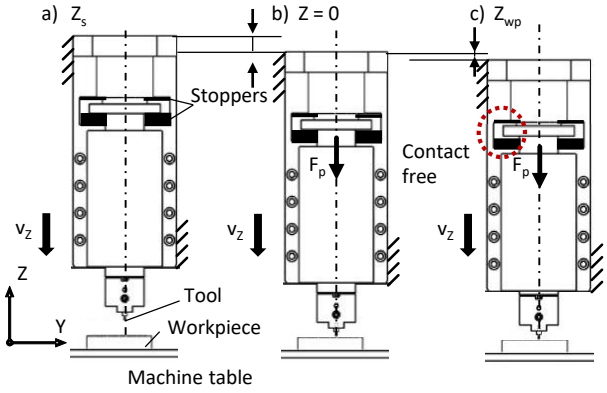

Figure 4. a) Safety position Z_s, b) contact position Z = 0 and c) embossing position Z_{wp}

2.2. Embossing tool specification

For the embossing process, tools of high strength and hardness are necessary to shape the workpiece within the specific form. The tool geometry is essential for generating the desired structures. A hard metal shaft with a corundum sphere (ruby-Al_2O_3) was used as tool for embossing concave optics. The ruby radius is R_r = 0.25 mm. The geometrical parameters of the tool and process are shown on Figure 5.

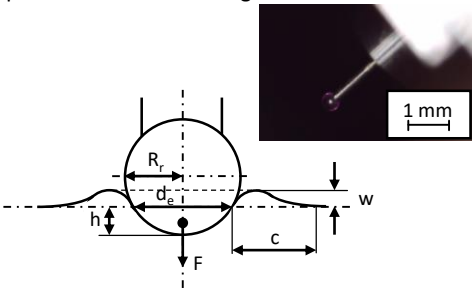

Figure 5. Geometrical parameters of the embossing tool

R_r stands for the tool radius and d_e for the embossings diameter. Those two parameters and the embossing depth h define the optic geometry. The aim of this manufacturing process is to produce a surface with low defect rate and as little pile-up as possible.

2.3. Embossing system set-up

Due to the non-linear behaviour of the VCA and the force sensor, both need to be investigated before the experiments. For this purpose, the force F has been determined for various positions Z_{wp} with a speed v_z = 30 mm/min. The interval set for the working point was ΔZ_{wp} = 150 µm, in range of 150 µm ≤ Z_{wp} ≤ 750 µm with a holding time t = 5 s. Figure 6 shows the force measurements N for the different embossing depths Z_{wp}.

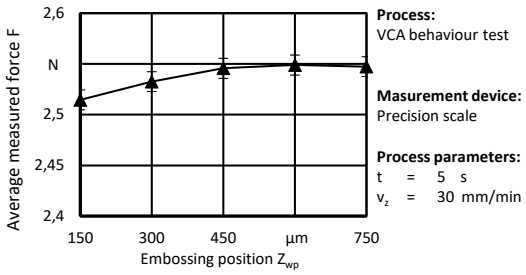

Figure 6. Force measurements N at different Z_{wp} positions

It was noticed that the force F in the range of 450 µm ≤ Z_{wp} ≤ 750 µm shows an almost constant behaviour. It is presumed that on the range of 150 µm ≤ Z_{wp} ≤ 450 µm, the plastic stopper suffers elastic deformations and by further increasing the embossing depth Z_{wp}, this deformation no longer influences the force F measurements. Therefore, the working position Z_{wp} = 600 µm is selected for the experiments.

The display resolution of the current measuring instrument has an uncertanty of u = 0.01 A. This affects the measured force with approx. uF(I) = 0.15 N. For the FTS, a current-force characteristic curve was defined using the measured values (Figure 7). A negative current indicates a Lorentz force of the VCA against the gravitational force and a positive current means a displacement on the direction of the gravitational force.

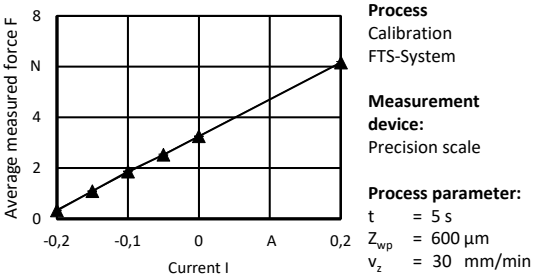

Figure 7. Current-force characteristic curve of the fast-tool-servo

The force sensor was used to determine embossing force F. In the measuring range, the values show a non-linear behavior from the force measured at the sensor to the force measured on the precision scale. For this reason, a 3rd degree polynomial is approximated. The measured values are shown in the mean value with the corresponding standard deviation in Figure 8 and used to correct the measured embossing forces.

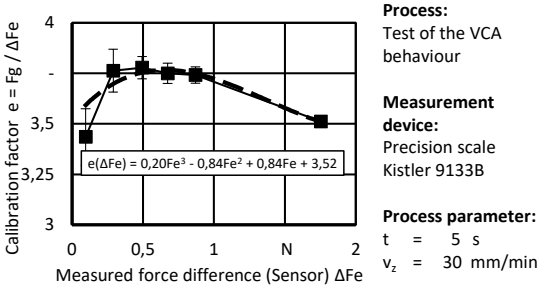

Figure 8. Difference of the force measured at the force sensor and the precision scale

3. Result

3.1. Variation of holding time, embossing speed and force

The main focus is to investigate how strongly the variation of embossing force F, holding time s and embossing speed v_z affect the geometry of embossed cavities. For this purpose, mean values of the individual stages are examined using the contrast method for the strength of effect they have on the overall process. Only the difference between these mean values is referred to as the effect. This gives a statement about the linearity of the factors on the result. The greater the effect of one factor in relation to the other effects, the greater the influence of this factor on the overall result. The effect diagrams of process parameters are shown in direct comparison in Figure 9.

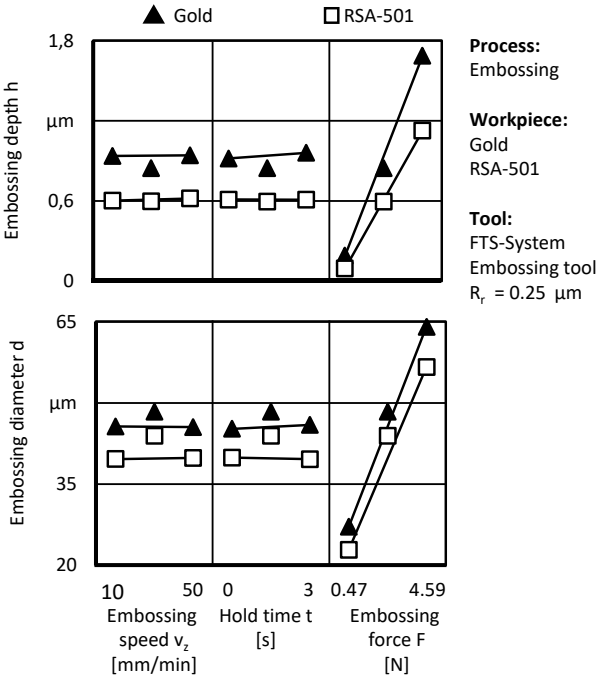

Figure 9. Effect diagram for the variation of embossing speed, hold time and embossing force F_p

3.2. Variation of embossing distance

To show the feasibility of the process, examples of micro-optical array in RSA-501 and gold were manufactured using the developed embossing system. The parameters are fixed in this execution, except for the embossing centre distance ΔX and the material. The investigation was carried out for gold and RSA-501. From the results of the previous investigation it is known that the embossing diameters amount to d ≈ 60 µm when the parameters are set as described above. To avoid overlapping the embossing cavities, an interval of 10 µm was set to a range of 60 µm ≤ ΔX ≤ 100 µm. For each characteristic, five embossings were carried out. In Figure 10, the experimental results are

shown. In Figure 12 the WLI measurement of the cavities and the measured profiles of them.

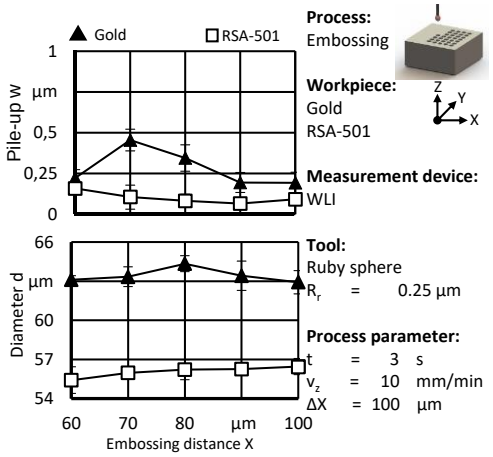

Figure 10. Embossing experiments result varying the embossing distance X

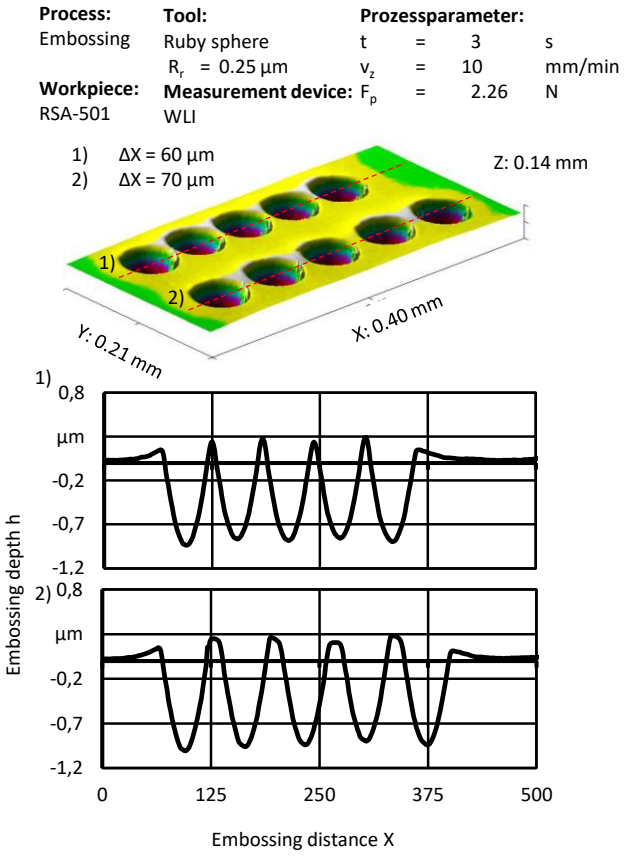

Figure 11 Example of micro-optical array manufacturing using the developed embossing system

4. Discussion and Outlook

At this investigation, the feasibility of using a FTS-system coupled at the ultra-precision machine tool was successfully implemented for embossing MOAs on gold and RSA-501. However, some considerations about the material properties of the surface and sub-surface zone of gold and RSA-501 have to be taken into account. For instance, an accurate method or process chain to prepare and induce a minimum of sub-surface and surface alterations on the workpiece. The aim of this process chain is to reduce the generated residual stresses and roughness of the substrate derived from previous cutting or preparation methods. Therefore, it will generate a more homogeneous workpiece, consequently dimishing the influence of the previous manufacturing method on the embossed MO geometry.

As expected, the embossings show pile-up at the edges. This behaviour can be minimized by a comprehensive analysis and understanding of the role of residual stresses caused by previous preparation methods. Additionally, it was shown that by increasing the distance between the embossings cavities, the pile-up effect was reduced. These experiments are of particular interest for manufacturing of high lens density MOAs.

Mostly, for embossing individual cavities, it was observed a strong dependency of the embossing force F_p, as expected, in contrast to hold time s and embossing speed v_z. This behaviour is expected as ductile materials such as aluminium and gold do not exhibit significant time dependent mechanical properties during indentation experiments. In future investigations, this process will be tested on materials such as amorph Nickel Phosphorus, in which the hold time s and embossing velocity v_z are presumed to play a stronger role on the material flow during the embossing process in comparison to gold and RSA-501.

For future developments and in order to increase the general knowledge about the process, models and simulation about the embossing process will be done. These methods are known for their accuracy and cost-effectiveness. For instance, Finite-Element (FE) simulation alongside analytical models can provide a proper description of the embossing process fo different tool geometries and embossing force F. However, it is important to take into consideration the effects of the micro size effect as described by POPOV [8]. Only then, the numeric results can be compared to measured experimental results.

Aknowledgement

The authors would like to aknowledge the company LT ULTRA-PRECISION TECHNOLOGY GMBH for providing the fast-tool-servo for the investigations.

References

[1] Herzig, H. P., *Micro-Optics: Elements, Systems and Applications*, Chapman and Hall/CRC, Boca Raton 2014.

[2] Klocke, F., *Fertigungsverfahren 1*, Springer Berlin Heidelberg, Berlin, Heidelberg 2008.

[3] Gerchman, M. C., in: Korsch, D. G. (Ed.), *Reflective Optics II*, SPIE 1989, p. 224.

[4] Rhorer, R.L., Evans, C.J. (Ed.), *Handbook of optics: Fabrication of optic by diamond turning*, McGraw-Hill, New York 2010.

[5] Brinksmeier, E., Riemer, O., Gläbe, R. M., *Fabrication of Complex Optical Components*, Springer Berlin Heidelberg, Berlin, Heidelberg 2013.

[6] Scheiding, S., Yi, A. Y., Gebhardt, A., Li, L., Risse, S., Eberhardt, R., Tünnermann, A., Freeform manufacturing of a microoptical lens array on a steep curved substrate by use of a voice coil fast tool servo. *Optics express* 2011, *19*, 23938–23951.

[7] Kirchberg, S., Chen, L., Xie, L., Ziegmann, G., Jiang, B., Rickens, K., Riemer, O., Replication of precise polymeric microlens arrays combining ultra-precision diamond ball-end milling and micro injection molding. *Microsyst Technol* 2012, *18*, 459–465.

[8] Popov, V. L., Method of reduction of dimensionality in contact and friction mechanics: A linkage between micro and macro scales. *Friction* 2013, *1*, 41–62.